

BELLCOMM, INC.

955 L'ENFANT PLAZA NORTH, S.W., WASHINGTON, D.C. 20024

N 69 40798
NASA CR-106457

COVER SHEET FOR TECHNICAL MEMORANDUM

TITLE- Dynamic Distortion of a
Gimbale Telescope

TM- 69-1022-3

FILING CASE NO(S)- 103-8

DATE- May 21, 1969

AUTHOR(S)- G. M. Anderson

FILING SUBJECT(S) Space Astronomy
(ASSIGNED BY AUTHOR(S))- Telescope Distortion
Crew Motion Induced Telescope Distortion
Timoshenko Beam Dynamics
ABSTRACT

The structural distortion of an orbiting telescope is determined for a suddenly applied ramp function of displacement of the gimbal resulting from a worst case astronaut impulsive translation. For a spacecraft the size of the Apollo Applications Orbital Workshop, this disturbance was found to produce a change in pointing direction due to telescope bending of from 0.5 to 2.0 seconds of arc. These values are large compared to stability requirements for a large orbiting telescope that may be more stringent than 0.1 seconds of arc.

Translational decoupling of the telescope from the spacecraft by means of springs is included in the analysis, and it was shown that this method can reduce dynamic distortion to any desired level, even below 0.01 seconds of arc.

The telescope structure is modeled as a prismatic beam and the Timoshenko beam equations are solved using the Laplace transformation for both the space and time variables. A proof is given that the integrand of the inversion integral is always single valued for beams of finite length. The residue theorem may therefore be applied without the need for integration around branch cuts.

The treatment of the applied load as a boundary condition in shear is employed in the analysis. This method has been the occasion of error and discussion in the literature. The relevant history is discussed with my assessment of the nature of the difficulty and its resolution.

**CASE FILE
COPY**

BA-145A (8-68)

SEE REVERSE SIDE FOR DISTRIBUTION LIST

DISTRIBUTION

COMPLETE MEMORANDUM TO

CORRESPONDENCE FILES:

OFFICIAL FILE COPY
plus one white copy for each
additional case referenced

TECHNICAL LIBRARY (4)

NASA Headquarters

Messrs. P. E. Culbertson/MLA
D. L. Forsythe/MLA
H. Glaser/SG
H. Hall/MTX
C. Janow/REC
T. A. Keegan/MA-2
J. L. Mitchell/SG
E. J. Ott/SG
H. J. Smith/SG
F. J. Sullivan/RE
Miss N. G. Roman/SG

Chrysler Space Division
(Michoud, La.)

Mr. D. N. Buell

GSFC

Messrs. K. L. Hallam/613
W. G. Stroud/110

Langley Research Center

Mr. W. W. Anderson/AMPD
W. E. Howell/FID
P. R. Kurzhals/AMPD

MSC

Messrs. R. G. Chilton/EG
W. B. Evans/KM
O. K. Garriott/CB
K. G. Henize/CB
R. O. Piland/TA
O. G. Smith/KF

COMPLETE MEMORANDUM TO, CONTINUED

MSFC

Messrs. M. Brooks/R-ASTR-NG
W. B. Chubb/R-ASTR-NGD
J. A. Downey/R-SSL-S
E. W. Ivey/R-P&VE-SLS
J. L. Mack/R-ASTR-S
F. B. Moore/R-ASTR-DIR
J. R. Olivier/R-AS-MO
H. L. Shelton/R-ASTR-FD
E. Stuhlinger/R-SSL-DIR

Perkin-Elmer

Messrs. H. Wischnia
A. B. Wissinger

Princeton University

Messrs. R. E. Danielson
M. Schwarzschild
L. Spitzer, Jr.

Sperry-Rand (Huntsville, Ala.)

Messrs. T. Gismondi
R. E. Skelton

Bellcomm

Messrs. F. G. Allen
A. P. Boysen
C. Buffalano
H. A. Helm
D. A. Chisholm
W. D. Grobman
D. R. Hagner
B. T. Howard
R. K. McFarland
J. Z. Menard
G. T. Orrok
I. M. Ross
R. V. Sperry
J. W. Timko
R. L. Wagner
D. B. Wood

Division 102
Department 1024 File
Central File

Table of Contents

	<u>Page</u>
I. INTRODUCTION	1
II. TIMOSHENKO BEAM DYNAMICS	2
III. TRANSLATIONAL DECOUPLING - RESPONSE TO ASTRONAUT IMPULSIVE TRANSLATION	11
IV. APPROXIMATION FOR STRONG DECOUPLING	17
V. POINT MASS LOADS - STRONG DECOUPLING	20
VI. NUMERICAL RESULTS	21
VII. CONCLUSIONS	25
ACKNOWLEDGEMENT	25
APPENDIX A	
Timoshenko Beam Analysis	A-1
APPENDIX B	
Properties of Space Eigen-values, $r_1(s)$ and $r_2(s)$	B-1
Proof that Integrand of Inversion Integral is Single Valued	B-8
APPENDIX C	
Ranges of Dimensionless Parameters	C-1

SUBJECT: Dynamic Distortion of a
Gimbaled Telescope
Case 103-8

DATE: May 21, 1969

FROM: G. M. Anderson

TM-69-1022-3

TECHNICAL MEMORANDUM

I. INTRODUCTION

Gimbal mounted telescopes carried on orbiting spacecraft are subject to structural deformation produced by attitude perturbations of the spacecraft if the telescope is not located at the spacecraft center of gravity.* The spacecraft will ordinarily have an attitude control system for limiting the effect of the principal environmental disturbances, however this system will usually be inadequate to fully cope with rapid internal disturbances such as those arising from crew motion. The resulting structural deformation of the telescope is doubtless quite small, but it may be of significance for high accuracy systems with pointing requirements more stringent than 0.1 arc seconds.

The dynamic distortion of a prismatic beam used to support a telescope is determined here for an extreme crew motion disturbance, i.e. an astronaut impulsive translation at the maximum distance from the spacecraft center of mass. The spacecraft, assumed to move as a rigid body, experiences a linear angular displacement which reaches a limit value at the time the astronaut reaches the opposite wall.

Timoshenko beam theory is employed to determine the distortion. The improvement which may be obtained by providing translational decoupling between the telescope beam and the spacecraft with a spring is included in the analysis.

The Laplace transformation is used for both space and time variables. The behavior of the two space eigenvalues are sketched on a closed contour in the s plane** around a typical cut. Although many of the functions have branch points,

* F. G. Allen has suggested that this effect may be important.

**The normalized time transform variable.

the integrand of the inversion integral is single valued and the residue theorem may be applied without integrating around branch cuts. A proof is offered that all Timoshenko beams of finite length enjoy this important property. A prior argument to this effect is felt to be deficient.*

It was found that for cases of strong translational decoupling the response is dominated by the static deflection. Static is a misnomer but it conveys well the idea that the beam response to very low frequency forcing functions, well below the lowest beam natural frequency, may be calculated using static principles. The load is of course the inertial loading of the beam mass. Once this was recognized it was a simple matter to include point mass loads, which is a welcome extension.

II. TIMOSHENKO BEAM DYNAMICS

In this section the response of a uniform prismatic beam is determined for an applied force at the center. Point mass loads are not considered. The Timoshenko⁽¹⁾ model includes the effects of rotary inertia and shear distortion. The development of the Timoshenko theory has been marked by some error and controversy. Some of this interesting history and a bibliography is given in Appendix A.

The notation and the evaluation of the shear coefficient are taken from Cowper.⁽²⁾ The Timoshenko equations are:

$$(a) \quad \frac{\partial Q}{\partial z} + p = \rho A \frac{\partial^2 w}{\partial t^2}$$

$$(b) \quad \frac{\partial M}{\partial z} - Q = \rho I \frac{\partial^2 \phi}{\partial t^2}$$

(1)

$$(c) \quad EI \frac{\partial \phi}{\partial z} = M$$

$$(d) \quad \frac{\partial w}{\partial z} + \phi = \frac{Q}{KAG}$$

*See pg. 15.

Notation:

- w - Mean deflection of cross section
 ϕ - Mean angle of rotation of a cross section about neutral axis
 Q - Total transverse shear force acting on a cross section
 p - Total transverse load per unit length applied to beam
 M - Bending moment acting at any cross section of beam
 A - Cross sectional area
 E - Modulus of elasticity
 F - Force spring exerts on beam
 G - Shear modulus
 I - Area moment of inertia
 K - Shear coefficient
 M_b - Total mass of beam
 M_t - Point mass at end of beam
 $Z(z,s)$ - Transfer impedance of beam
 $a = (\ell/2) \sqrt{\rho/E}$ - Limiting transit time for waves on the half beam
 $b = \sqrt{E/\rho}$ - One of two limiting velocities. Other is $b/\sqrt{\pi_1}$.
 $d_n(\zeta)$ - ζ variation of nth mode of $\delta\eta_+(\zeta,\tau)$
 $e_n(\zeta)$ - ζ variation of nth mode of $\delta\phi_+(\zeta,\tau)$
 k - Spring constant
 ℓ - Beam length
 r - Normalized space transform variable
 s - Normalized time transform variable
 t - Time
 t_1 - Time for ramp function to reach value x_m .
 $u(t)$ - Heaviside unit step function.
 x_v - Displacement of spacecraft at gimbal
 x_m - Displacement of spacecraft in time t_1 .
 z - Distance along axis of beam
 ρ - Mass density of beam

ω_n = nth normalized natural circular frequency of beam

$$\Omega_b = 2\pi f_b = 1/a$$

$$\Omega_{bs} = \sqrt{k/M_t} = 2\pi f_{bs} \text{ - Circular frequency of rigid telescope spring system}$$

Normalized Variables

$$f = F/(KAG)$$

$$\tau = t/a$$

$$\xi = 2x_v/\ell$$

$$\xi_m = 2x_m/\ell$$

$$\eta = 2w/\ell$$

$$\zeta = 2z/\ell$$

$$\delta\eta = \eta(\zeta, \tau) - \eta(1, \tau) \text{ - Distortion index}$$

$$\delta\phi = \phi(\zeta, \tau) \text{ - Distortion index}$$

$$\delta\eta_{+m} = |\delta\eta_+(0, \tau)|_{\max}$$

$$\delta\phi_{+m} = |\delta\phi_+(0, \tau)|_{\max}$$

Dimensionless Parameters

$$\pi_1 = E/(KG)$$

$$\pi_2 = 4I/(A\ell^2)$$

$$\pi_3 = \frac{4}{\ell} \frac{EA}{K} = \left(\frac{\Omega_b}{\Omega_{bs}}\right)^2 = \left(\frac{f_b}{f_{bs}}\right)^2$$

Subscripts

Plus (+) and minus (-) on forcing or response functions refer to the corresponding positive or negative ramp functions of Figure 2.

A single bar over a variable indicates the time transform; two bars indicate time and space transforms.

Figure 1 is a schematic of the beam and the elastic coupling to the spacecraft.

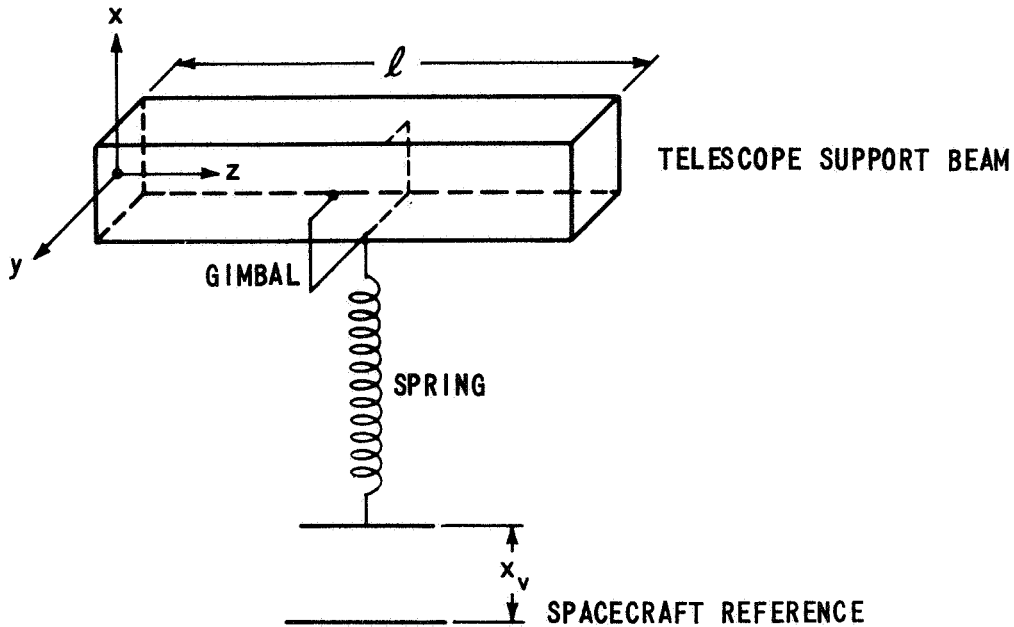


FIGURE 1

It is assumed that the attitude variations of the spacecraft may be considered as translational motion of the gimbal. Further, since these motions occur in a time small compared to the orbital period, the orbital motion may be neglected and the spacecraft and telescope considered nominally at rest.

The method employed divides the beam at the center, $z=l/2$, and considers one half of the spring force applied as a shear load to each side of the beam. The problem is thus reduced to the homogeneous condition with $p(z,t)=0$ and the following boundary conditions for the left half of the beam:

$$z=0; \quad \partial \phi / \partial z = 0, \quad \frac{\partial w}{\partial z} + \phi = 0$$

(2)

$$z=l/2; \quad \phi = 0, \quad \frac{\partial w}{\partial z} + \phi = \frac{F}{2 KAG}$$

Eliminating M and Q from Equations (1), one obtains

$$(a) \quad \rho A \frac{\partial^2 W}{\partial t^2} - KAG \left(\frac{\partial^2 W}{\partial z^2} + \frac{\partial \phi}{\partial z} \right) = 0$$

(3)

$$(b) \quad \rho I \frac{\partial^2 \phi}{\partial t^2} - EI \frac{\partial^2 \phi}{\partial z^2} + KAG \left(\frac{\partial W}{\partial z} + \phi \right) = 0$$

as coupled equations in w and ϕ .

Introducing the dimensionless parameters and normalized variables defined in the notation yields, for Equations (3),

$$(a) \quad \pi_1 \frac{\partial^2 \eta}{\partial \tau^2} - \frac{\partial^2 \eta}{\partial \zeta^2} - \frac{\partial \phi}{\partial \zeta} = 0$$

(4)

$$(b) \quad \pi_1 \pi_2 \frac{\partial^2 \phi}{\partial \tau^2} - \pi_1 \pi_2 \frac{\partial^2 \phi}{\partial \zeta^2} + \frac{\partial \eta}{\partial \zeta} + \phi = 0$$

with boundary conditions

$$\zeta = 0; \quad \frac{\partial \phi}{\partial \zeta} = 0, \quad \frac{\partial \eta}{\partial \zeta} + \phi = 0$$

(5)

$$\zeta = 1; \quad \phi = 0, \quad \frac{\partial \eta}{\partial \zeta} + \phi = \frac{f}{2}$$

The time and space transforms used are

$$(6) \quad \bar{\eta}(\zeta, s) = \int_0^{\infty} e^{-s\tau} \eta(\zeta, \tau) d\tau$$

and

$$(7) \quad \bar{\eta}(r, s) = \int_0^{\infty} e^{-r\zeta} \bar{\eta}(\zeta, s) d\zeta$$

with similar relations for ϕ .

The beam is considered to be initially at rest. Transform Equations (4) and (5) with respect to τ to obtain

$$(a) \quad \pi_1 s^2 \bar{\eta}(\zeta, s) - \frac{d^2 \bar{\eta}(\zeta, s)}{d\zeta^2} - \frac{d\bar{\phi}(\zeta, s)}{d\zeta} = 0$$

(8)

$$(b) \quad \pi_1 \pi_2 s^2 \bar{\phi}(\zeta, s) - \pi_1 \pi_2 \frac{d^2 \bar{\phi}(\zeta, s)}{d\zeta^2} + \frac{d\bar{\eta}(\zeta, s)}{d\zeta} + \bar{\phi}(\zeta, s) = 0$$

$$(a) \quad \bar{\phi}_{\zeta}(0, s) = 0; \quad \bar{\eta}_{\zeta}(0, s) + \bar{\phi}(0, s) = 0$$

(9)

$$(b) \quad \bar{\phi}(1, s) = 0; \quad \bar{\eta}_{\zeta}(1, s) + \bar{\phi}(1, s) = \frac{\bar{f}(s)}{2}$$

and the ζ subscript indicates the corresponding derivative.

Transform Equations (8) with respect to ζ using boundary conditions (9a) to obtain

$$(\pi_1 s^2 - r^2) \bar{\eta} - r \bar{\phi} = -r \bar{\eta}(0, s)$$

(10)

$$\left(\frac{r}{\pi_1 \pi_2}\right) \bar{\eta} + \left(s^2 - r^2 + \frac{1}{\pi_1 \pi_2}\right) \bar{\phi} = \left(\frac{1}{\pi_1 \pi_2}\right) \bar{\eta}(0, s) - r \bar{\phi}(0, s)$$

Equations (10) are solved for $\bar{\eta}$ and $\bar{\phi}$ to yield

$$\bar{\eta}(r, s) = \frac{r(r^2 - s^2) \bar{\eta}(0, s) - r^2 \bar{\phi}(0, s)}{D(r)}$$

(11)

$$\bar{\phi}(r, s) = \frac{(s^2/\pi_2) \bar{\eta}(0, s) + r(r^2 - \pi_1 s^2) \bar{\phi}(0, s)}{D(r)}$$

where

$$(12) \quad D(r) = r^4 - (\pi_1 + 1)s^2 r^2 + (s^2/\pi_2)(1 + \pi_1 \pi_2 s^2)$$

$$= (r^2 - r_1^2)(r^2 - r_2^2)$$

$$(13) \quad r_1 = \left[(s/2) \left\{ (\pi_1 + 1) s + \sqrt{(\pi_1 - 1)^2 s^2 - 4/\pi_2} \right\} \right]^{1/2}$$

$$(14) \quad r_2 = \left[(s/2) \left\{ (\pi_1 + 1) s - \sqrt{(\pi_1 - 1)^2 s^2 - 4/\pi_2} \right\} \right]^{1/2}$$

The properties of r_1 and r_2 as functions of s are given in Appendix B.

The unknown constants $\bar{\eta}(0, s)$ and $\bar{\phi}(0, s)$ are evaluated using the boundary conditions (9b) after first inverting Equations (11) relative to r . Either the inverse transform

$$(15) \quad \bar{\eta}(\zeta, s) = \frac{1}{2\pi j} \int_{c-j\infty}^{c+j\infty} e^{r\zeta} \bar{\eta}(r, s) dr$$

with c real, positive, and larger than real part of all roots of $D(r)$ or tables may be used to determine $\bar{\eta}(\zeta, s)$ and $\bar{\phi}(\zeta, s)$. The inversion of $\bar{\eta}(\zeta, s)$ and $\bar{\phi}(\zeta, s)$ involve terms

$$L^{-1} \frac{1}{D(r)} = \frac{1}{(r_1^2 - r_2^2)} \left\{ \frac{1}{r_1} \sinh r_1 \zeta - \frac{1}{r_2} \sinh r_2 \zeta \right\}$$

$$L^{-1} \frac{r}{D(r)} = \frac{1}{(r_1^2 - r_2^2)} \left\{ \cosh r_1 \zeta - \cosh r_2 \zeta \right\}$$

(16)

$$L^{-1} \frac{r^2}{D(r)} = \frac{1}{(r_1^2 - r_2^2)} \left\{ r_1 \sinh r_1 \zeta - r_2 \sinh r_2 \zeta \right\}$$

$$L^{-1} \frac{r^3}{D(r)} = \frac{1}{(r_1^2 - r_2^2)} \left\{ r_1^2 \cosh r_1 \zeta - r_2^2 \cosh r_2 \zeta \right\}$$

where L^{-1} indicates the inversion process of (15).

The inversion of Equations (11), using relations (16), gives

$$\bar{\eta}(\zeta, s) = \frac{1}{(r_1^2 - r_2^2)} \left\{ G_1(\zeta, s) \bar{\eta}(0, s) + H_1(\zeta, s) \bar{\phi}(0, s) \right\}$$

(17)

$$\bar{\phi}(\zeta, s) = \frac{1}{(r_1^2 - r_2^2)} \left\{ G_2(\zeta, s) \bar{\eta}(0, s) + H_2(\zeta, s) \bar{\phi}(0, s) \right\}$$

where

$$\begin{aligned}
 G_1(\zeta, s) &= (r_1^2 - s^2) \cosh r_1 \zeta - (r_2^2 - s^2) \cosh r_2 \zeta \\
 H_1(\zeta, s) &= - \left\{ r_1 \sinh r_1 \zeta - r_2 \sinh r_2 \zeta \right\} \\
 (18) \\
 G_2(\zeta, s) &= (s^2 / \pi_2) \left\{ \frac{1}{r_1} \sinh r_1 \zeta - \frac{1}{r_2} \sinh r_2 \zeta \right\} \\
 H_2(\zeta, s) &= - \left\{ (r_2^2 - s^2) \cosh r_1 \zeta - (r_1^2 - s^2) \cosh r_2 \zeta \right\}
 \end{aligned}$$

The symmetry of Equations (18) has been enhanced by the use of the relation

$$r_1^2 + r_2^2 = (\pi_1 + 1) s^2$$

from Equation (12).

Introducing $\bar{\eta}_\zeta(1, s)$ and $\bar{\phi}(1, s)$ from Equations (17) into boundary conditions (9b) gives*

$$\begin{aligned}
 \bar{\eta}(0, s) &= \frac{(r_1^2 - r_2^2) B_2(s)}{2 S(s)} \bar{f}(s) \\
 (19) \\
 \bar{\phi}(0, s) &= - \frac{(r_1^2 - r_2^2) A_2(s)}{2 S(s)} \bar{f}(s)
 \end{aligned}$$

Substituting $\bar{\eta}(0, s)$ and $\bar{\phi}(0, s)$ from (19) into (17) gives

* $A_2(s)$, $B_2(s)$ and $S(s)$ are defined on p. 11.

$$(a) \quad \bar{\eta}(\zeta, s) = \frac{1}{2} \frac{P(\zeta, s)}{S(s)} \bar{f}(s)$$

(20)

$$(b) \quad \bar{\phi}(\zeta, s) = \frac{1}{2} \frac{R(\zeta, s)}{S(s)} \bar{f}(s)$$

where

$$(a) \quad P(\zeta, s) = G_1(\zeta, s) B_2(s) - H_1(\zeta, s) A_2(s)$$

$$(b) \quad R(\zeta, s) = G_2(\zeta, s) B_2(s) - H_2(\zeta, s) A_2(s)$$

$$(c) \quad S(s) = A_1(s) B_2(s) - A_2(s) B_1(s)$$

$$(21) \quad (d) \quad A_1(s) = r_1 (r_1^2 - s^2) \sinh r_1 - r_2 (r_2^2 - s^2) \sinh r_2$$

$$(e) \quad B_1(s) = - \left\{ r_1^2 \cosh r_1 - r_2^2 \cosh r_2 \right\}$$

$$(f) \quad A_2(s) = -G_2(1, s)$$

$$(g) \quad B_2(s) = -H_2(1, s)$$

III. TRANSLATIONAL DECOUPLING - RESPONSE TO ASTRONAUT IMPULSIVE TRANSLATION

So far the analysis has been developed for an applied force at the center of the beam. The results may be easily extended to include the effect of the decoupling spring. The spring force $F(t)$ is related to the displacements by

$$F(t) = k \{x_v(t) - w(\ell/2, t)\}$$

or, in normalized variables

$$(22) \quad f(\tau) = \frac{2\pi_1}{\pi_3} \left\{ \xi(\tau) - \eta(1, \tau) \right\}$$

Transform Equation (22) with respect to τ and employ Equation (20a) to obtain

$$\frac{\pi_1}{\pi_3} \bar{\eta}(1, s) + \frac{\bar{f}(s)}{2} = \frac{\pi_1}{\pi_3} \bar{\xi}(s)$$

(23)

$$\bar{\eta}(1, s) - Z(1, s) \frac{\bar{f}(s)}{2} = 0,$$

where

$$Z(\zeta, s) = \frac{\bar{\eta}(\zeta, s)}{\bar{f}(s)/2} = \frac{P(\zeta, s)}{S(s)}$$

is the mechanical transfer impedance of the half beam.

From Equations (23)

$$(24) \quad \frac{\bar{f}(s)}{2} = \frac{\bar{\xi}(s)}{Z(1, s) + (\pi_3/\pi_1)}$$

Substitute $\bar{f}(s)/2$ from (24) into (20) to obtain

$$(a) \quad \bar{\eta}(\zeta, s) = \frac{P(\zeta, s)}{Q(s)} \bar{\xi}(s)$$

(25)

$$(b) \quad \bar{\phi}(\zeta, s) = \frac{R(\zeta, s)}{Q(s)} \bar{\xi}(s)$$

where

$$(26) \quad Q(s) = P(1, s) + (\pi_3/\pi_1) S(s)$$

It is necessary to determine $\xi(s)$ for the prescribed spacecraft displacement. Figure 2 indicates the spacecraft rigid body motion resulting from an astronaut impulsive translation. As explained previously, such a translation maneuver results in an angular perturbation of the spacecraft which, for present purposes, may be considered as a translation at the spring.

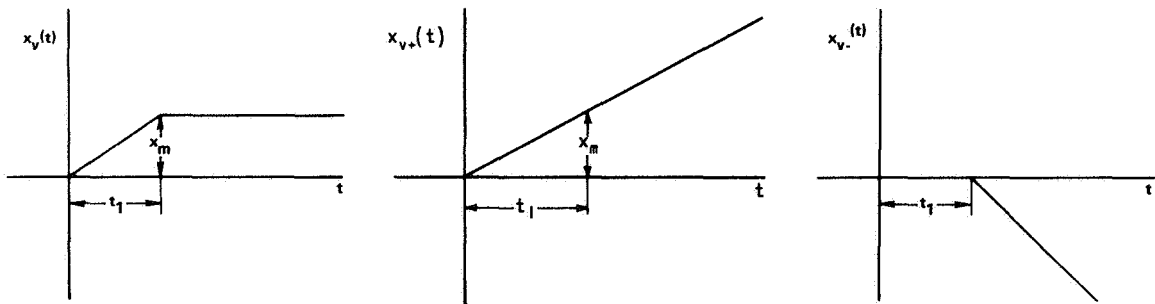


Figure 2

A convenient method of dealing with the function of Figure 2 is to consider it made up of two ramps functions

$$(27) \quad x_v = x_{v+}(t) + x_{v-}(t)$$

where

$$x_{v+}(t) = x_m \frac{t}{t_1} u(t)$$

$$(28) \quad x_{v-}(t) = -x_{v+}(t-t_1)$$

$$u(t) = 0 \quad , \quad t < 0$$

$$= 1 \quad , \quad t \geq 0$$

The corresponding response functions are

$$(29) \quad \eta(\zeta, \tau) = \eta_+(\zeta, \tau) + \eta_-(\zeta, \tau)$$

$$\phi(\zeta, \tau) = \phi_+(\zeta, \tau) + \phi_-(\zeta, \tau)$$

where

$$\eta_-(\zeta, \tau) = -\eta_+(\zeta, \tau - \tau_1)$$

$$\phi_-(\zeta, \tau) = -\phi_+(\zeta, \tau - \tau_1)$$

Normalizing $x_{v+}(t)$, one obtains

$$\xi_+(\tau) = \left(\frac{a}{t_1}\right) \xi_m \tau$$

which has a time transform

$$(30) \quad \bar{\xi}_+(s) = \left(\frac{a}{t_1}\right) \frac{\xi_m}{s^2}$$

The response functions are given by

$$(a) \quad \eta_+(\zeta, \tau) = \frac{1}{2\pi j} \int_{c-j\infty}^{c+j\infty} e^{s\tau} \bar{\eta}_+(\zeta, s) ds$$

(31)

$$(b) \quad \phi_+(\zeta, \tau) = \frac{1}{2\pi j} \int_{c-j\infty}^{c+j\infty} e^{s\tau} \bar{\phi}_+(\zeta, s) ds$$

It is shown in Appendix B that the integrands of (31) are single valued for beams of finite length and the residue theorem may therefore be used.* The singularities are simple poles on the imaginary s axis, where

$$Q(s) = 0 \quad ; \quad s \neq 0$$

It may be shown that

$$\lim_{s \rightarrow 0} \frac{P(\zeta, s)}{Q(s)} = 1$$

and

$$\lim_{s \rightarrow 0} \frac{R(\zeta, s)}{Q(s)} = \frac{(1-\zeta^3)}{3!} \frac{s^2}{\pi_2}$$

With these results, and using Equations (25) and (30), Equations (31) may be written

*Leonard and Budiansky⁽¹⁶⁾ claim that this conclusion follows from the uniqueness of the solution to the differential equation. This reason appears inadequate in view of the fact that infinite beam problems do have multiple valued integrands^(5,10).

$$(a) \quad \eta_+(\zeta, \tau) = \left(\frac{a}{t_1}\right) \xi_m \tau - 2j \left(\frac{a}{t_1}\right) \xi_m \sum_{n=1}^{\infty} \frac{P(\zeta, j\omega_n)}{\omega_n^2 Q'(j\omega_n)} \sin \omega_n \tau$$

(32)

$$(b) \quad \phi_+(\zeta, \tau) = -2j \left(\frac{a}{t_1}\right) \xi_m \sum_{n=1}^{\infty} \frac{R(\zeta, j\omega_n)}{\omega_n^2 Q'(j\omega_n)} \sin \omega_n \tau$$

where

$$s_n = j\omega_n$$

is nth root of

$$Q(s) = 0$$

and

$$Q'(j\omega_n) = \left. \frac{dQ(s)}{ds} \right|_{s=j\omega_n}$$

Distortion

Two measures of telescope distortion are defined:

$$\delta \eta(\zeta, \tau) = \eta(\zeta, \tau) - \eta(1, \tau)$$

(33)

$$\delta \phi(\zeta, \tau) = \phi(\zeta, \tau) - \phi(1, \tau) = \phi(\zeta, \tau)$$

IV. APPROXIMATION FOR STRONG DECOUPLING

As might be expected, Equations (32) can be much simplified if

$$\omega_2 \ll \omega_1$$

where ω_1 is the frequency of the rigid body beam-spring mode and ω_2 is the first natural frequency of the beam.

Let

$$\delta \eta_+(\zeta, \tau) = \xi_m \left(\frac{a}{t_1}\right) \sum_{n=1}^{\infty} d_n(\zeta) \sin \omega_n \tau$$

(34)

$$\delta \phi_+(\zeta, \tau) = \xi_m \left(\frac{a}{t_1}\right) \sum_{n=1}^{\infty} e_n(\zeta) \sin \omega_n \tau$$

where

$$d_n(\zeta) = -2j \left[\frac{P(\zeta, j\omega_n) - P(1, j\omega_n)}{\omega_n^2 Q'(j\omega_n)} \right]$$

(35)

$$e_n(\zeta) = -2j \left[\frac{R(\zeta, j\omega_n) - R(1, j\omega_n)}{\omega_n^2 Q'(j\omega_n)} \right]$$

Figures (3) and (4) plot the error in the peak distortion, using the first term in the series (34),

$$(36) \quad \Delta \delta \eta_{+m} = 1 - \frac{d_1(0)}{\sum_1^{10} d_n(0)}$$

$$\Delta \delta \phi_{+m} = 1 - \frac{e_1(0)}{\sum_1^{10} e_n(0)}$$

where the summation is limited to ten terms.* The dashed lines show that the error in using the first term is dependent on (ω_2/ω_1) for the 16:1 range of π_2 considered. The effect of π_1 will be shown later to be small so that these plots may be taken as indicative of the region in which the rigid-body frequency dominates the distortion.

The distortion indices for strong decoupling are therefore

$$(37) \quad \delta \eta_{+}(\zeta, \tau) \cong \xi_m \left(\frac{a}{t_1}\right) d_1(\zeta) \sin \omega_1 \tau$$

$$\delta \phi_{+}(\zeta, \tau) \cong \xi_m \left(\frac{a}{t_1}\right) e_1(\zeta) \sin \omega_1 \tau$$

Expanding about $s=0$, one obtains, from (18) and (21)

$$P(\zeta, s) \cong (\mu_1^2 - \mu_2^2) \left[-1 + \left\{ \left(\frac{1}{\pi_2}\right) \left(\frac{\zeta^4}{4!} - \frac{\zeta}{3!} + 1\right) - \frac{1}{2!}(\pi_1 \zeta^2 + 1) \right\} s^2 \right]$$

*Data for Figures (1) and (2) are from a computer program. Ten terms are more than adequate for engineering accuracy.

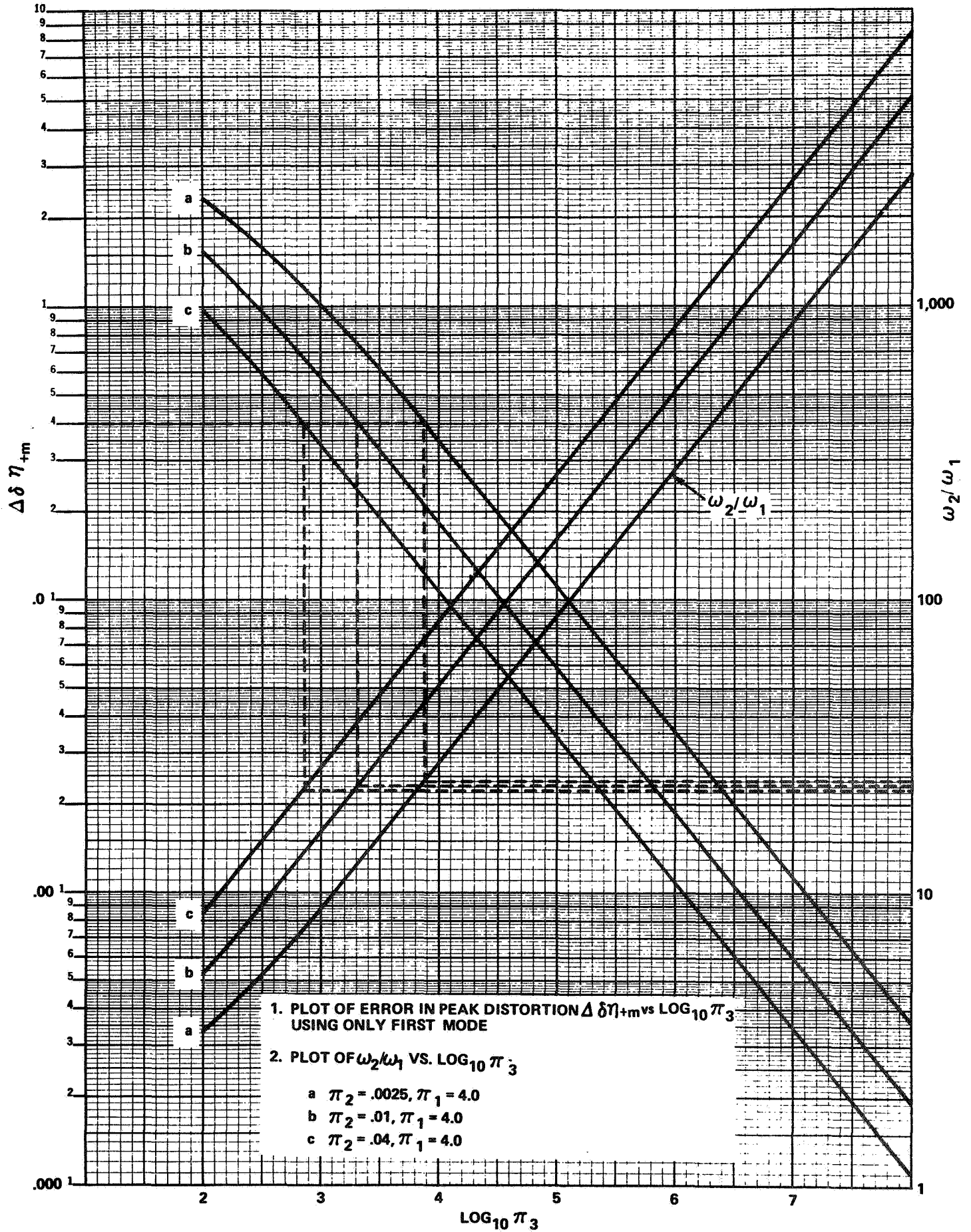


FIGURE 3

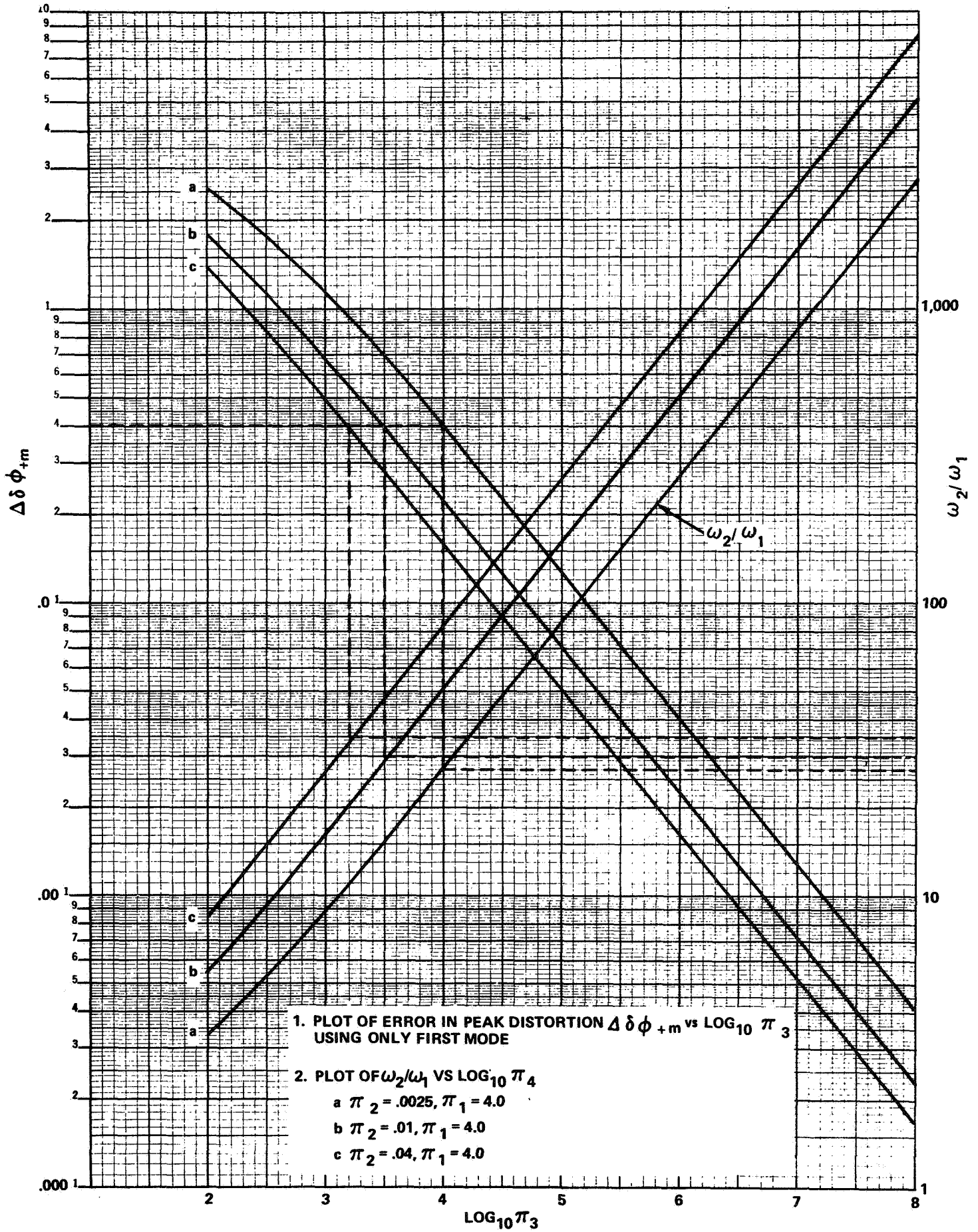


FIGURE 4

$$(38) \quad R(\zeta, s) \cong (\mu_1^2 - \mu_2^2) \left(\frac{1}{3!}\right) \left(\frac{1}{\pi_2}\right) (1 - \zeta^3) s^2$$

$$S(s) \cong -\pi_1 (\mu_1^2 - \mu_2^2) s^2$$

Substituting from Equations (38) into the characteristic equation

$$(39) \quad Q(s) = P(1, s) + \left(\frac{\pi_3}{\pi_1}\right) S(s) = 0$$

one finds

$$\omega_1 \cong \frac{1}{\sqrt{\pi_3}}$$

which is exactly the rigid body frequency.

Setting $s = j\omega_1$ in Equations (38) using Equations (35) gives, for $\zeta = 0$

$$d_1(0) = \frac{1}{\sqrt{\pi_3}} \left\{ \frac{1}{8\pi_2} + \frac{\pi_1}{2} \right\}$$

(40)

$$e_1(0) = \frac{1}{3!} \left(\frac{1}{\pi_2}\right) \frac{1}{\sqrt{\pi_3}}$$

$Q'(j\omega_1)$ is obtained from Equation (39).

The total distortion indices, considering the positive and negative ramp functions, for $\zeta = 0$, $\tau > 0$, are

$$\delta \eta(0, \tau) \cong \xi_m \left(\frac{a}{t_1} \right) d_1(0) \left\{ \sin \omega_1 \tau - u(\tau - \tau_1) \sin \omega_1 (\tau - \tau_1) \right\}$$

$$\delta \phi(0, \tau) \cong \xi_m \left(\frac{a}{t_1} \right) e_1(0) \left\{ \sin \omega_1 \tau - u(\tau - \tau_1) \sin \omega_1 (\tau - \tau_1) \right\}$$

These approximations turn out to be identical with results obtained using static principles. In this method the beam is presumed to be subjected to a uniform inertial load which is due to the vibration at the frequency ω_1 . The calculation is extremely simple and direct.*

V. POINT MASS LOAD - STRONG DECOUPLING

The static method may be used to determine the distortion for the case of strong decoupling. The results are

$$d_1(0) = \frac{1}{\sqrt{\pi_4}} \left[\frac{\pi_1}{2} \left\{ 1 + 2\gamma \right\} + \frac{1}{24\pi_2} \left\{ 3 + 8\gamma \right\} \right]$$

$$e_1(0) = \frac{1}{6\pi_2 \sqrt{\pi_4}} \left[1 + 3\gamma \right]$$

where

$$\gamma = \frac{M_t}{M_b/2} = \frac{2M_b}{M_b}$$

These results are for a mass M_t at each end of the beam and a total beam mass of M_b . The terms $d_1(0)$ and $e_1(0)$ play the same role as the corresponding expressions in Equations (41).

From Equations (42), the point mass loads produce 2 to 2 2/3 times the deflection and 3 times the plane rotation of the equivalent beam mass.

*Preston Smith carried through the static analysis both for this case and for the results given in Section V which includes equal point mass loads at the ends of the beam.

VI. NUMERICAL RESULTS

The parameter ranges of interest, derived in Appendix C, are summarized here.

$$\pi_1 = E/KG$$

The range is

$$2.33 < \pi_1 < 6.76$$

for cross sections with symmetry about x and y axes. Computer runs were normally made for values 2.0, 4.0, 6.0 and 8.0 which bracket the range.

$$\pi_2 = 4I/A\ell^2$$

Again restricting consideration to cases with x and y axis symmetry, the range is

$$1/4 (d/\ell)^2 < \pi_2 < 2/3 (d/\ell)^2$$

where d is maximum dimension normal to z axis.

$$\pi_3 = (4/\ell) (EA/k)$$

This parameter is an approximate index of decoupling since

$$\begin{aligned} \pi_3 &= (\Omega_b/\Omega_{bs})^2 \\ &= (f_b/f_{bs})^2 \end{aligned}$$

where

$$\begin{aligned} \Omega_b &= 2\pi f_b = 1/a \\ \Omega_{bs} &= \sqrt{k/M_b} \end{aligned}$$

The parameter π_3 is not a precise index of decoupling since Ω_b is not an eigen-frequency of the beam in bending. However, increasing π_3 , for constant beam parameters, does lower f_{bs} and hence increase decoupling.

The lower limit on f_{bs} may be set in one of two ways. Clearly

$$f_{bs} > 1/T$$

where T is the orbital period. As f_{bs} is reduced, gravity-gradient will induce larger amplitude periodic motion which must be accommodated. In consequence of these considerations there is an upper limit on π_3 which must be determined for a practical design. Thus

$$0 < \pi_3 < \pi_{3max}$$

There appears to be adequate range for π_3 to provide all of the decoupling desired without getting into design extremes.*

$$\frac{\xi_m a}{t_1}$$

It is not necessary to treat these quantities parametrically since the results may be presented as a ratio of $\delta\eta$ and $\delta\phi$ to $(a/t_1) \xi_m$. However, to obtain an estimate of distortion, values of these parameters are required.

For a vehicle the size of the Apollo Applications Program Orbital Workshop, using a rigid body model and conservation of angular momentum, it is possible to show that

$$\frac{x_m}{t_1} < .1 \text{ inch/sec.}$$

with a peak excursion which is less than 1 inch. This estimate is based on a worst case astronaut translation from one side of the Workshop to the other at the maximum distance from the mass center at a velocity of 3 ft./sec.

*This subject will be developed by J. Schindelin in a forthcoming memorandum.

For the aluminum beam example of Appendix C

$$\begin{aligned} \left(\frac{a}{t_1}\right) \xi_m &= \left(\frac{1}{\Omega_b t_1}\right) \left(\frac{2x_m}{\ell}\right) = \left(\frac{2}{\ell}\right) \left(\frac{1}{\Omega_b}\right) \left(\frac{x_m}{t_1}\right) \\ &= (10^{-2}) \left(\frac{1}{2\pi \times 320}\right) \quad (.1) \\ &= .5 \times 10^{-6} \end{aligned}$$

Distortion

A computer program was developed to compute $\delta\eta$ and $\delta\phi$. Some results from this program are given here for the case of no decoupling. The distortion extremes

$$\frac{\delta\eta_{+m}}{\xi_m a/t_1} = \sum_1^{10} |d_n(0)|$$

$$\frac{\delta\phi_{+m}}{\xi_m a/t_1} = \sum_1^{10} |e_n(0)|$$

are given in Tables I-IV for

$$\pi_1 = 2.0, 4.0, 6.0, 8.0$$

$$\pi_2 = .0025, .01, .04$$

$$\pi_3 = 0$$

The tables also give the branch point locations and the first ten natural frequencies.

From Tables I-IV, it is found that

$$1.4 \times 10^{-6} < \delta\eta_{+m} < 5 \times 10^{-6}$$

$$0.5 < \delta\phi_{+m} < 2.0, \text{ secs. of arc}$$

for $(a/t_1) \xi_m = 0.5 \times 10^{-6}$.

It is adequate to deal with $\delta\eta_+$ and $\delta\phi_+$ in this instance since the beam frequencies are large compared to $(1/t_1)$ and the maximum will occur before the effect of the negative ramp function is felt. Note that the effect of π_1 on the distortion is slight.

Numerical results for strong decoupling, obtained from Equations (40) and (41), show for $\pi_3 = 10^4$,

$$.02 \times 10^{-6} < \delta\eta_{+m} < .27 \times 10^{-6}$$

$$.0041 < \delta\phi_{+m} < .069 \text{ secs. of arc}$$

for $(a/t_1) \xi_m = 0.5 \times 10^{-6}$.

This value of π_3 is relatively modest since it requires

$$\frac{f_b}{f_{bs}} = 100$$

or

$$f_{bs} = .01 f_b$$

$$= 3.2 \text{ Hz}$$

for the example beam of Appendix C.

Further reduction in $\delta\eta_{+m}$ and $\delta\phi_{+m}$ can be made by increasing π_3 . The falloff will go as π_3 instead of $\sqrt{\pi_3}$ for

$$f_{bs} \ll 1/t_1,$$

the additional reduction coming from $\sin \omega_1 \tau$ in Equation 37 since ω_1 decreases as π_3 increases.

By way of reference, the spring travel for a natural frequency of 3.2 Hz is about 4×10^{-6} inches due to gravity-gradient in low earth orbit. The amplitude increases as $(1/f_{bs})^2$ so there is considerable latitude for reducing f_{bs} before spring travel becomes troublesome.

VII. CONCLUSIONS

The pointing degradation of the telescope to structural distortion can be inferred by examining $\delta\phi$. This parameter controls the change in orientation of one end of the beam, the probable location of the major optical element, since in this model the beam center does not rotate.

1. For large spacecraft, of the size of the Apollo Applications Orbital Workshop, worst case crew motion impulsive translations can lead to values of $\delta\phi$, and hence to variations in telescope pointing directions, of from 0.5 to 2.0 seconds of arc. These values assume no point mass loading and cover a fairly wide range of material and geometrical variations. These estimates may be increased several times if actual, i.e. point mass, loads are considered. In any case these values are large compared to stability requirements of 0.1, or less, seconds of arc.
2. Translational decoupling of the telescope and its support structure from the spacecraft offers one approach for reducing the effects of crew motion on pointing stability to negligible proportions, even below 0.01 seconds of arc.

ACKNOWLEDGEMENT

I wish to acknowledge the considerable support provided by Nancy Kirkendall in this study. She not only did a creative job on the computer program but she also checked the analysis and corrected the algebraic errors.

My colleagues Preston Smith, Jack Kranton, William Hough and Robert Ravera read the draft manuscript and offered numerous helpful suggestions. Preston Smith's probing questions of the beam eigen-frequencies led to the discovery that the computer program was sometimes missing the first mode. This in turn led to the simplifications for strong decoupling.



G. M. Anderson

1022-GMA-mef

Attachments
References
Tables I-IV
Appendixes

REFERENCES

1. "On the Correction for Shear of the Differential Equation for Transverse Vibrations of Prismatic Bars," by S. P. Timoshenko, Philosophical Magazine, Vol. 41, 1921, pp 744-746.
2. "The Shear Coefficient in Timoshenko's Beam Theory," by G. R. Cowper, Journal of Applied Mechanics, Vol. 33, June 1966, pp 335-340.
3. "Influence of Rotary Inertia and Shear on Flexural Motions of Isotropic Elastic Plates," R. D. Mindlin, Journal of Applied Mechanics, Vol. 18, pp 31-38, 1951.
4. "The Propagation of Waves in the Transverse Vibrations of Beams and Plates," by Ya. S. Uflyand, Prikladnaya Matematika i Mekhanika, Vol. 12, May-June, 1948, pp 287-300 (In Russian).
5. "Transverse Impact of Long Beams, Including Rotary Inertia and Shear Effects," by M. A. Dengler and M. Goland, Proceedings of First U. S. National Congress of Applied Mechanics, 1951, pp 179-186.
6. "Flexural Wave Solutions of Coupled Equations Representing the More Exact Theory of Bending," by J. Miklowitz, Journal of Applied Mechanics, Vol. 20, 1953, pp 511-514.
7. "On Traveling Waves In Beams," by R. W. Leonard and B. Budiansky, NACA TR 1173, 1954.
8. "Propagation of Elastic Impact in Beams in Bending," by M. Goland, P. D. Wickenshorn, and M. A. Dengler, Journal of Applied Mechanics, Vol. 22, March 1955, pp 1-7.
9. "Some Solutions of the Timoshenko Beam Equation for Short Pulse-Type Loading," by H. J. Plass, Jr., Journal of Applied Mechanics, Vol. 25, September 1958, pp 379-385.
10. "Traveling Force on a Timoshenko Beam," by A. L. Florence, Journal of Applied Mechanics, Vol. 32, June 1965, pp 351-358.

11. "Normal Modes of Oscillation of Beams," by C. L. Dolph Willow Run Research Center, University of Michigan, UMM-79, October 1950, 18 pages.
12. "Flexural Vibrations in Uniform Beams According to the Timoshenko Theory," by R. A. Anderson, Journal of Applied Mechanics, Vol. 20, December 1953, pp 504-510.
13. "The Effect of Rotatory Inertia and of Shear Deformation on the Frequency and Normal Mode Equations of Uniform Beams with Simple End Conditions," by T. C. Huang, Journal of Applied Mechanics, Vol. 28, December 1961, pp 579-584.
14. Ibid p 37.
15. "Flexural Wave Solution of Coupled Equations Representing the More Exact Theory of Bending," Discussion by M. A. Dengler, Journal of Applied Mechanics, Vol. 21, June 1954, pp 204-205.
16. Ibid p 17.

Table I

$\pi_1 = .2000+01$

$\pi_3 = .0000$

		π_2	
		.2500-02	.1000-01
			.4000-01
$\delta \eta_{+m} / (\xi_m a / t_1)$.1010+02	.5176+01
$\delta \phi_{+m} / (\xi_m a / t_1)$ radians		.1925+02	.9539+01
$\delta \phi_{+m} / (\xi_m a / t_1)$ secs. of arc		.3971+07	.1967+07
C_1		.4000+02	.2000+02
C_2		.1414+02	.7071+01
ω_1		.1728-00	.3299-00
ω_2		.9892-00	.1575+01
ω_3		.2478+01	.3513+01
ω_4		.4292+01	.5492+01
ω_5		.6296+01	.7442+01
ω_6		.8397+01	.7956+01
ω_7		.1054+02	.9565+01
ω_8		.1266+02	.1018+02
ω_9		.1454+02	.1189+02
ω_{10}		.1475+02	.1266+02

Table II

$\pi_1 = .4000+01$

$\pi_3 = .0000$

		π_2	
		.2500-02	.1000-01
			.4000-01
$\delta \eta_{+m} / (\xi_m a / t_1)$.1027+02	.5454+01
$\delta \phi_{+m} / (\xi_m a / t_1)$ radians		.1906+02	.9354+01
$\delta \phi_{+m} / (\xi_m a / t_1)$ secs. of arc.		.3931+07	.1929+07
C_1		.1333+02	.6667+01
C_2		.1000+02	.5000+01
ω_1		.1709-00	.3174-00
ω_2		.9307-00	.1366+01
ω_3		.2231+01	.2936+01
ω_4		.3724+01	.4391+01
ω_5		.5314+01	.5598+01
ω_6		.6926+01	.6241+01
ω_7		.8519+01	.7342+01
ω_8		.9909+01	.8117+01
ω_9		.1068+02	.9519+01
ω_{10}		.1127+02	.9913+01

Table III

$$\pi_1 = .6000+01 \quad \pi_2 = .0000$$

	.2500-02	.1000-01	.4000-01
$\delta \eta_{+m} / (\xi_m a / t_1)$.1042+02	.5691+01	.3563+01
$\delta \phi_{+m} / (\xi_m a / t_1)$ radians	.1889+02	.9149+01	.4129+01
$\delta \phi_{+m} / (\xi_m a / t_1)$ secs. of arc.	.3896+07	.1887+07	.8517+06
C_1	.8000+01	.4000+01	.2000+01
C_2	.8165+01	.4082+01	.2041+01
ω_1	.1691-00	.3061-00	.4690-00
ω_2	.8812-00	.1226+01	.1414+01
ω_3	.2048+01	.2582+01	.2621+01
ω_4	.3337+01	.3761+01	.3131+01
ω_5	.4680+01	.4679+01	.4399+01
ω_6	.6013+01	.5375+01	.5118+01
ω_7	.7308+01	.6383+01	.5787+01
ω_8	.8305+01	.6873+01	.6970+01
ω_9	.8980+01	.8148+01	.8133+01
ω_{10}	.9549+01	.8879+01	.8319+01

Table IV

$$\pi_1 = .8000+01 \quad \pi_2 = .0000$$

	.2500-02	.1000-01	.4000-01
$\delta \eta_{+m} / (\xi_m a / t_1)$.1056+02	.5915+01	.3855+01
$\delta \phi_{+m} / (\xi_m a / t_1)$ radians	.1872+02	.8995+01	.3929+01
$\delta \phi_{+m} / (\xi_m a / t_1)$ secs. of arc.	.3862+07	.1855+07	.8104+06
C_1	.5714+01	.2857+01	.1429+01
C_2	.7071+01	.3536+01	.1768+01
ω_1	.1673-00	.2958-00	.4337-00
ω_2	.8390-00	.1125+01	.1293+01
ω_3	.1905+01	.2333+01	.2352+01
ω_4	.3051+01	.3348+01	.2769+01
ω_5	.4229+01	.4116+01	.3846+01
ω_6	.5381+01	.4779+01	.4813+01
ω_7	.6493+01	.5815+01	.5196+01
ω_8	.7284+01	.6123+01	.6071+01
ω_9	.7936+01	.7136+01	.7189+01
ω_{10}	.8509+01	.8139+01	.8029+01

APPENDIX A

Timoshenko Beam Analysis

Timoshenko beam theory occupies the middle ground between the classical, Euler-Bernoulli theory, and the exact but relatively intractable formulation of elasticity theory. An excellent account of the evolution of the Timoshenko theory and a discussion of its merits is given by Mindlin.⁽³⁾

Both travelling wave⁽³⁻¹⁰⁾ and modal analyses⁽¹¹⁻¹³⁾ have been used for the solution of problems. The choice depends on the nature of the problem. Mindlin⁽³⁾ gives an elegant proof that the Timoshenko equations, in the absence of distributed loads, reduce to a set of wave equations.

In this paper the modal method is the appropriate formulation since the time of wave propagation over the beam length is small compared to the duration of the excitation. The load is considered as a shear boundary condition. This method was used erroneously by Uflyand.⁽²⁾ Dengler and Goland⁽³⁾ pointed out Uflyand's boundary conditions are incompatible. They do not identify the error, however, but avoid it by adopting the method which treats the load as an applied δ function on a continuous beam.

Miklowitz⁽⁶⁾ returns to the boundary condition method. He uses a formulation of the Timoshenko equations that treats the total deflection as the sum of bending plus shear components as

$$y = y_b + y_s$$

The shear deflection is defined as

$$y_s = \partial \phi / \partial z$$

Miklowitz claims advantages of simplicity (he means algebraically) plus less chance of pitfalls with the difficult boundary conditions.

The algebraic advantages may be real in some problems. They did not prove so in the problem treated here.

The boundary condition advantage is not a real one. Miklowitz has an error of a factor of 2 in his boundary condition, Equation 13, where he writes

$$\frac{\partial y_s(0,t)}{\partial x} = - \frac{S(0,t)}{k'A_0G}$$

and $S(0,t)$ is the shear load at $x=0$. This should read $S/2$ for S . Miklowitz's result, Equation (16), is in error by the same factor and does not check Dengler and Goland's result as asserted.

Dengler in his discussion of Miklowitz's paper claims that it may be demonstrated without difficulty that

$$y_x(0,t) = 0$$

The demonstration is not given. Miklowitz in his closure objects, and rightly, since the Dengler condition is clearly wrong.

In view of the prior difficulty with the shear load treated as a boundary condition at a cut, it has seemed useful to review the history. The difficulties appear to stem from a lack of recognition of the discontinuity of the derivative, $\partial w/\partial z$ in the notation of this paper, at the cut. Thus the load is considered to be equally divided between the two halves of the beam.

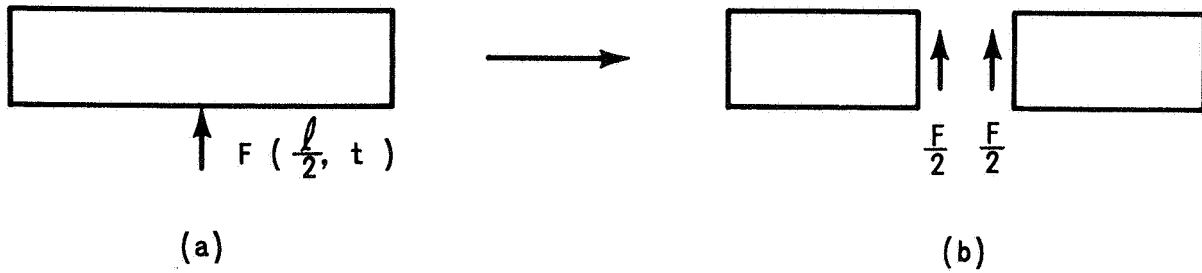


FIGURE (A-1)

In (b) above the shear load $F/2$ is applied to the right hand face of the left half beam and

$$\left. \frac{\partial w}{\partial z} \right|_{\frac{l}{2}^-} = \frac{+F}{2 KAG}$$

and on the right half beam

$$\left. \frac{\partial w}{\partial z} \right|_{\frac{l}{2}^+} = \frac{-F}{2 KAG}$$

Everyone agrees that $\phi(l/2, t) = 0$, or $y_{bx}(0, t) = 0$ in the notation of the coupled equations, so there is no difficulty on that score.

APPENDIX B

This Appendix considers two matters:

1. Branch points of $r_1(s)$ and $r_2(s)$, and
2. Proof that the integrand of the final inversion integral is single valued for beams of finite length.

Branch Points of $r_1(s)$

This function defined in Equation (13) as

$$r_1(s) = \left[(s/2) \left\{ (\pi_1+1)s + \sqrt{(\pi_1-1)^2 s^2 - 4/\pi_2} \right\} \right]^{1/2}$$

has three branch points all of order 1/2. They are

(a) $s = 0$

(B-1)

(b) $s = \pm c_1 = \pm \frac{2}{(\pi_1-1)\sqrt{\pi_2}}$

where c_1 is real and positive. The branch points at $\pm c_1$ come from the zero of the radical internal to the brackets {}.

Near $s=0$

(B-2) $r_1(s) \approx \frac{j^{1/2}}{\sqrt[4]{\pi_2}} \sqrt{s} = \lambda_{10} \sqrt{s}$

Near $s = c_1$, let $s_1 = s - c_1$; $s = s_1 + c_1$; $|s_1| \ll c_1$

then

$$(B-3) \quad r_1(s_1) \approx c_1 \sqrt{\frac{\pi_1+1}{2}} \left\{ 1 + \left(\frac{\pi_1-1}{\pi_1+1} \right) \sqrt{\frac{2s_1}{c_1}} \right\}$$

$$(B-4) \quad = r_{11} + \lambda_{11} \sqrt{s_1}$$

with a similar result near $-c_1$.

Figure (B-1) below shows the correspondence between the $r_1(s)$ and s planes on a contour surrounding a suitable cut. The cut in the s plane runs from $-c_1$ to $+c_1$ along the real s axis.

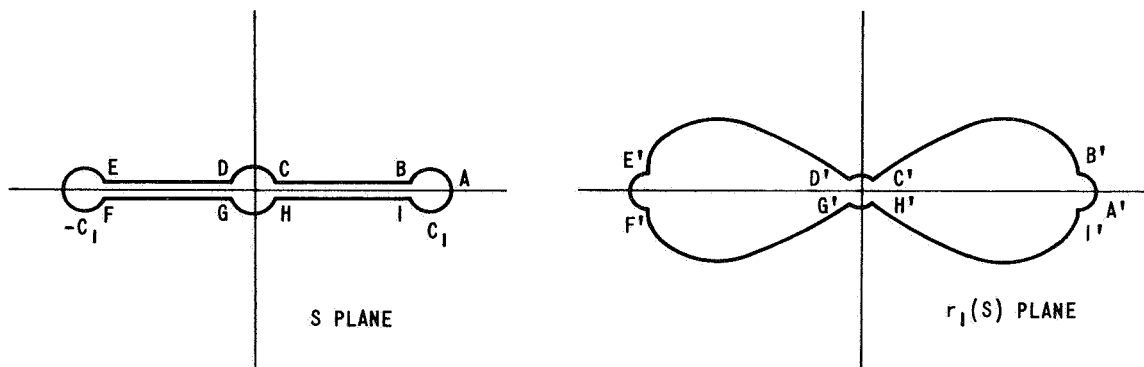


FIGURE B-1

Branch Points of $r_2(s)$

This function, from Equation (14),

$$r_2(s) = \left[(s/2) \left\{ (\pi_1+1) s - \sqrt{(\pi_1-1)^2 s^2 - 4/\pi_2} \right\} \right]^{1/2}$$

has five branch points, all of order 1/2. They are

$$\begin{aligned} \text{(a)} \quad & s = 0 \\ \text{(B-5) (b)} \quad & s = \pm c_1 = \pm \frac{2}{(\pi_1-1)\sqrt{\pi_2}} \\ \text{(c)} \quad & s = \pm jc_2 = \pm j/\sqrt{\pi_1\pi_2} \end{aligned}$$

where c_1 and c_2 are real and positive. c_1 has the same value as in Equation (B-1b) as it originates from the same source. c_2 is associated with the zero of the brackets $\{\}^{1/2}$.

Near $s=0$

$$\text{(B-6)} \quad r_2(s) \approx \frac{j^{3/2}\sqrt{s}}{4\sqrt{\pi_2}} = \lambda_{20}\sqrt{s}$$

Near $s = c_1$, again let $s_1 = s - c_1$; $|s_1| \ll c_1$

then

$$r_2(s_1) \approx c_1 \sqrt{\frac{\pi_1+1}{2}} \left\{ 1 - 1/2 \left(\frac{\pi_1-1}{\pi_1+1} \right)^2 \sqrt{\frac{2s_1}{c_1}} \right\}$$

$$(B-7) \quad r_2(s_1) = r_{11}(s_1) - \lambda_{21} \sqrt{s_1}$$

with again a similar result near $-c_1$.

$$\text{Near } s = jc_2, \text{ let } s_2 = s - jc_2; \quad |s_2| \ll c_2$$

then

$$(B-8) \quad r_2(s_2) \approx \left[\left(\frac{jc_2}{2} \right) \left\{ (\pi_1 + 1)(s_2 + jc_2) - \lambda \left(1 + \frac{jc_2(\pi_1 - 1)s_2}{\lambda^2} \right) \right\} \right]^{1/2}$$

where

$$\lambda^2 = (\pi_1 - 1)^2 (jc_2)^2 - 4/\pi_2$$

Using Equation (B-5c), one finds

$$(B-9) \quad r_2(s_2) \approx \lambda_{22} \sqrt{s_2}$$

where

$$\lambda_{22} = \sqrt{jc_2/2} \left\{ (\pi_1 + 1) - \frac{jc_2(\pi_1 - 1)}{\lambda} \right\}$$

Figure (B-2) shows the correspondence between $r_2(s)$ and s planes on a contour surrounding a suitable cut. The cut in this instance is a double one from $-c_1$ to $+c_1$ on the real s axis and from $-jc_2$ to $+jc_2$ on the imaginary s axis.

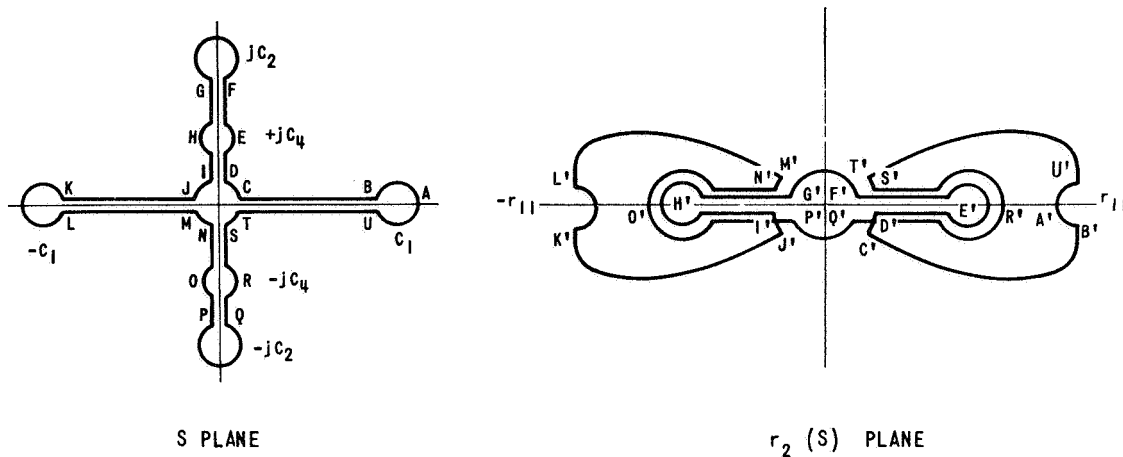


FIGURE B-2

The branches of $r_1(s)$ and $r_2(s)$ have been chosen so that as

$$(a) \quad \begin{matrix} s \rightarrow \infty \\ r_1(s) \rightarrow \sqrt{\pi_1} s \end{matrix}$$

B-10

$$(b) \quad r_2(s) \rightarrow s$$

In the light of this behavior at infinity, the reader may be perplexed, as I was, at the behavior of $r_2(s)$ at $s=c_1$. How can the contour A'B' start to the left of r_{11} and still retain $r_2(s) \rightarrow s$ as $s \rightarrow \infty$?

This effect can be explained with the aid of Figure B-3 below.

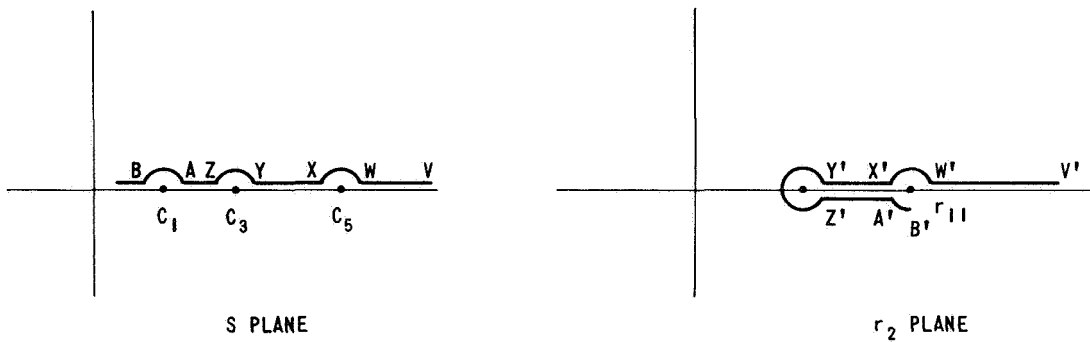


FIGURE B-3

There is a critical point* at

(B-11) $s = c_3 > c_1$ c_3 real and positive

*A critical point is where $r'(s)=0$. At these points the transformation $r(s)$ is not conformal.

on the real axis, and a corresponding point at $s=-c_3$. Given Equation (B-10b) and (B-11) it follows that there is a point

$$s = c_5 > c_3$$

such that

$$r_2(c_5) = r_2(c_1)$$

There are two additional critical points on the imaginary s axis at

$$s = \pm jc_4 \quad c_4 \text{ real and positive}$$

where

$$c_4 < c_2$$

as indicated in Figure (B-2).

An interesting property of $r_2(s)$ is evident in Figure (B-2). For those cases where

$$Q(s) = 0$$

has roots in range

$$-jc_2 < s < +jc_2$$

$r_2(s)$ will have real values. Outside this range $r_2(s)$ is always imaginary for s imaginary. Thus both hyperbolic and trigonometric functions appear simulataneously and this condition exists in the problem studied here. Some of the cases discussed by Huang⁽¹³⁾ fall into this category as well.

Integrand of Inversion Integral is Single Valued for Beams of Finite Length

The proof is based on the form of Equations (16). All of the functions there are even in both r_1 and r_2 . Since the beam response is a linear combination of these functions, it follows that the integrand of the inversion integral is even in r_1 and r_2 .

At the three points

$$s = 0$$

and

$$s = \pm jc_2$$

$$r(s) \approx \lambda \sqrt{\Delta s}$$

$$\Delta s = \Delta s ; s = 0$$

$$\Delta s = s - c_1 ; s = c_1$$

$$\Delta s = s + c_1 ; s = -c_1$$

where r stands for either r_1 or r_2 and λ any of the proportionality constants previously given for these points. It is clear that any even function of r will behave as

$$E[r(s)] \approx a_0 + a_1 \Delta s$$

in the vicinity of these three branch points. These functions are therefore single valued and the integrand is as well.

The points

$$s = \pm c_1$$

are more difficult. All the individual functions in r_1 or r_2 in Equations 16 do have branch points at $s = \pm c_1$.

Consider a typical term

$$\begin{aligned} \cosh r_1 \zeta - \cosh r_2 \zeta &\approx \left\{ \cosh r_{11} \zeta + \lambda_{11} \sqrt{s_1} \sinh r_{11} \zeta \right\} \\ &- \left\{ \cosh r_{11} \zeta - \lambda_{11} \sqrt{s_1} \sinh r_{11} \zeta \right\} \\ &= 2\lambda_{11} \sqrt{s_1} \sinh r_{11} \zeta \end{aligned}$$

using (B-4) and (B-7).

Also

$$r_1^2 - r_2^2 \approx 4 r_{11} \lambda_{11} \sqrt{s_1}$$

Therefore

$$\frac{1}{(r_1^2 - r_2^2)} \left\{ \cosh r_1 \zeta - \cosh r_2 \zeta \right\} \approx \frac{1}{2r_{11}} \sinh r_{11} \zeta$$

Equations (16) all exhibit the same property and the points $s = \pm c_1$ are therefore not branch points of the integrand of the inversion integral.

In this proof that $s = \pm c_1$ are not branch points of the integrand it has been necessary to have all of the four roots of $D(r) = 0$,

$$r = \pm r_1(s), \pm r_2(s)$$

Discarding any of these roots, as for example is required in infinite beam problems to satisfy the conditions at ∞ , voids the proof and such problems require integration around branch cuts (5,10).

BELLCOMM, INC.

APPENDIX C

Ranges of Dimensionless Parameters

$$\underline{\pi_1} = E/KG$$

The range of the parameter π_1 depends on K and ν since

$$\frac{E}{G} = 2(1+\nu)$$

where ν is Poisson's ratio. From the formulae in Reference (2), π_1 has been computed for a number of beam cross sections. The results are shown in Table C-I.

Table C-I

	π_1		
	$\nu=0$	$\nu=.3$	$\nu=.5$
Circle	2.33	2.93	3.33
Rectangle	2.40	3.06	3.50
Thin Walled Tube	4.00	4.90	5.50
Thin Walled Square Tube	4.80	5.96	6.76

* $m=2$; $n=1$; $t_F/t_w=1.0$ from Reference (2).

The corresponding values of K are given in Table C-II.

Table C-II

K

	$\nu=0$	$\nu=.3$	$\nu=.5$
Circle	.857	.886	.900
Rectangle	.833	.850	.857
Thin Walled Tube	.500	.531	.545
Thin Walled Square Tube	.417	.436	.444

$$\pi_2 = \frac{4I}{A\ell^2}$$

The following formulae apply to the indicated cross sections.

Circle	$\pi_2 = 1/4 (d/\ell)^2$
Rectangle	$\pi_2 = 1/3 (d/\ell)^2$
Thin Walled Round Tube	$\pi_2 = 1/2 (d/\ell)^2$
Thin Walled Square Tube	$\pi_2 = 2/3 (d/\ell)^2$

Thus

$$1/4 (d/\ell)^2 \leq \pi_2 \leq 2/3 (d/\ell)^2$$

where d is maximum dimension normal to axis for which I is computed.

If we assume that $d < .25\ell$, the maximum value of π_2 is

$$\pi_{2\max} = .04$$

The limits of π_2 are thus

$$0 < \pi_2 < .04$$

$$\underline{\pi_3 = (4/\ell)(EA/k)}$$

Let Ω_{bs} designate the natural circular frequency of the telescope spring system assuming the telescope to be rigid. Then

$$\begin{aligned} \Omega_{bs} &= \sqrt{k/M_b}, \text{ where } M_b = \rho A \ell \text{ is beam mass} \\ \pi_3 &= (4/\ell) \left(\frac{EA}{\Omega_{bs}^2 M_b} \right) \\ &= (4/\ell) \left(\frac{EA}{\Omega_{bs}^2 \rho A \ell} \right) \\ &= (1/a^2) / \Omega_{bs}^2 \\ &= (\Omega_b / \Omega_{bs})^2 \\ &= (f_b / f_{bs})^2 \end{aligned}$$

$$\text{where } \Omega_b = 2\pi f_b = 1/a.$$

As an example consider an aluminum beam with

$$\ell = 200 \text{ inches}$$

$$E = 10^7 \text{ lbs./sq.in.}$$

$$\rho = 2.47 \times 10^{-4} \text{ lb.sec}^2/\text{in}^4$$

which gives

$$f_b = 320 \text{ Hz.}$$